PERGAMON

Mechatronics 11 (2001) 27–42

MECHATRONICS

Optimal design and development of a five-bar finger with redundant actuation

Jae Hoon Lee[a], Byung-Ju Yi[a,*], Sang-Rok Oh[b], Il Hong Suh[a]

[a]*School of Electrical Engineering and Computer Science, Hanyang University, 1271 Sa 1-dong, Ansan, Kyungki, 425-791, South Korea*

[b]*Intelligent System Control Research Center, KIST, PO Box 131, Cheongryang, Seoul, South Korea*

Received 9 September 1998; received in revised form 1 October 1999; accepted 10 October 1999

Abstract

In order to develop a human hand mechanism, a five-bar finger with redundant actuation is designed and implemented. Each joint of the finger is driven by a compact actuator mechanism having an ultrasonic motor and a gear set with a potentiometer, and controlled by a VME bus-based control system. Optimal sets of actuator locations and link lengths for cases of a minimum actuator, one-, two-, and three-redundant actuators are obtained by employing a composite design index which simultaneously considers several performance indices, such as workspace, isotropic index, and force transmission ratio. According to the optimization result, several finger-configurations optimized for a special performance index are illustrated, and it is concluded that the case of one redundant actuator is the most effective in comparison to the cases of more redundant actuators, and that the case of two redundant actuators is the most effective in multi-fingered operation in which the force characteristic is relatively important, as compared to the kinematic isotropy and the workspace of the system.

1. Introduction

Robot hands have been employed for fine motion control and assembling parts. Most of the existing robot hands employ tendon-driven power transmission [1–4].

* Corresponding author. Fax: +82-345-416-6416.
E-mail address: bj@email.hanyang.ac.kr (B.-J. Yi).

0957-4158/01/$ - see front matter
PII: S0957-4158(99)00089-6

However, frictions existing in the transmission line require more effort on control. In light of this fact, we propose a five-bar finger mechanism which is directly driven by an ultra-sonic motor at the joints of the mechanism. Since the five-bar finger mechanism has many potential input locations for attaching actuators, a redundant actuation mode can be achieved [6,7]. Redundant actuation prevails in general biomechanical systems, such as the human body, and the bodies of mammals and insets [5]. Redundant actuation can also be found in many robotic applications. They include multiple arms, dual arms, multi-fingered hands, walking machines, and so on. Several load distribution criteria associated with load sharing and internal load generation have been developed by many researchers [6–12]. In the case of redundant actuation, the location and number of the actuator are very important parameters for the system performance.

Redundant actuation can be easily explained in terms of mobility. Mobility of a system is defined as the number of independent variables which must be specified in order to locate its elements relative to another. It is described by

$$M = D(L-1) - \sum_{i=1}^{J}(N - F_i), \tag{1}$$

where D, L, J, and F_i denote the degree-of-freedom of the rigid body (e.g. three in planar motion, six in spatial motion), the number of links, the number of joints, and the motion degree-of-freedom of the ith joint, respectively. When M is greater than N (operational or task-space degree-of-freedom), the system is called "*a kinematically redundant system*". On the other hand, when the number of actuators is greater than M (this situation usually happens in a closed-chain system), the system is called "*a redundantly actuated system*". For example, the mobility of the human upper-extremity (arm) can be considered as seven, while it has 29 human actuators (i.e., muscles). Accordingly, it has 22 redundant actuators.

The purpose of this paper is the optimum design and development of a five-bar finger employing ultra-sonic motors. Optimal sets of actuator locations and link lengths for the cases of using a minimum number of actuators, one-, two-, or three-redundant actuators, are obtained by employing a composite design index which simultaneously considers several performance indices, such as workspace, isotropic index, and force transmission ratio. According to the optimization result, several finger-configurations optimized for the special performance index are illustrated, and it is concluded that the case of one redundant actuator is the most effective in comparison to the cases of more redundant actuators and that the case of two redundant actuators is the most effective in a multi-fingered operation, in which the force characteristic is relatively important in the expense of the small workspace.

2. Kinematic modeling

The modeling methodology integrates the *Generalized Principle of D'Alembert* with the method of kinematic influence coefficients (KIC), resulting in closed form vector expressions. The reader is referred to Freeman and Tesar [14] for a more detailed description of the following scheme. In the following, the letter G stands for a first-order KIC matrix, and superscribed quantities indicate dependent parameters with subscripts denoting independent parameters.

2.1. Open-chain kinematics

Consider a five-bar finger mechanism shown in Fig. 1. This system has one closed-kinematic chain. The closed-kinematic chain is formed by connecting the two open-chains at the given location of the second link of the left open-chain, as shown in Fig. 1. In order to enlarge the area encompassed by the finger, the folded-in configuration of the right open-chain is chosen. Since the two kinematic chains of the five-bar mechanism have a common kinematic relation at the end-point of the system, the components of the end-point vector **u** are described by

$$x = l_1 c_1 + l_2 c_{12} = l_3 c_3 + l_4 c_{34} + l_5 c_{345} + a, \tag{2}$$

$$y = l_1 s_1 + l_2 s_{12} = l_3 s_3 + l_4 s_{34} + l_5 s_{345}, \tag{3}$$

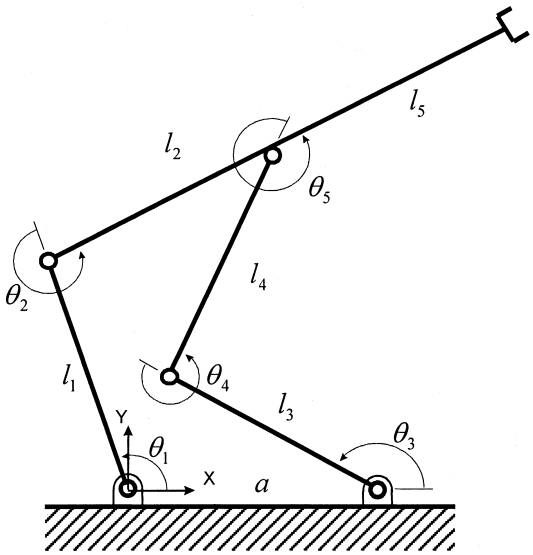

Fig. 1. Five-bar finger mechanism.

and

$$\Phi = \theta_1 + \theta_2 = \theta_3 + \theta_4 + \theta_5. \tag{4}$$

Adopting the standard Jacobian representation for the velocity of a vector of N dependent (output) parameters $\dot{\mathbf{u}}$ in terms of a set of P independent input coordinates ${}_r\dot{\phi}$ of the rth open-chain, one has

$$\dot{\mathbf{u}} = [{}_rG^u_\phi]{}_r\dot{\phi}_a. \tag{5}$$

Here,

$$[{}_rG^u_\phi] = \left[\frac{\partial u}{\partial_r\phi_1}, \frac{\partial u}{\partial_r\phi_2}, \ldots, \frac{\partial u}{\partial_r\phi_p}\right] \tag{6}$$

is the Jacobian relating the coordinates $\dot{\mathbf{u}}$ to ${}_r\dot{\phi}$, and is of dimension $N \times P$, with the mth column being of dimension $N \times 1$.

2.2. Internal kinematics for a five-bar finger mechanism

Since the mobility of this mechanism is two, at least two actuators are required to control the mechanism. There exist several choices in the selection of independent joints (i.e., actuator locations). In general, the base joints have been chosen as the actuator locations in previously developed five-bar systems, primarily to minimize the dynamic effect due to floating actuators. However, from a kinematic point of view, inclusion of one or two floating actuators may be promising. For example, a better manipulability, isotropy, or load handling capacity can be achieved by using a certain floating actuator [6]. An internal kinematic relationship between dependent joints and independent joints is required to deal with the problem addressed in the above.

The equivalent velocity relation is given by

$$\dot{\mathbf{u}} = [{}_1G^u_\phi]{}_1\dot{\phi} = [{}_2G^u_\phi]{}_2\dot{\phi}. \tag{7}$$

Choosing the joints θ_1 and θ_3 as the independent joint set ($\dot{\phi}_a$) and the joints θ_2, θ_4, and θ_5 as the dependent joint set ($\dot{\phi}_p$), Eq. (7) can be rearranged according to the following form

$$[A]\dot{\phi}_p = [B]\dot{\phi}_a, \tag{8}$$

where

$$[A] = [-[{}_1G^u_\phi]_{;2} \quad [{}_2G^u_\phi]_{;2,\,3}], \tag{9}$$

$$[B] = [[{}_1G^u_\phi]_{;1} \quad -[{}_2G^u_\phi]_{;1}], \tag{10}$$

$$\dot{\phi}_p = (\dot{\theta}_2 \quad \dot{\theta}_4 \quad \dot{\theta}_5)^{\mathrm{T}}, \tag{11}$$

and

$$\dot{\phi}_a = (\dot{\theta}_1 \quad \dot{\theta}_3)^{\mathrm{T}}. \tag{12}$$

Now, premultiplying the inverse of the matrix $[A]$ to both sides of Eq. (8) yields [13]

$$\dot{\phi}_p = [G_a^{\ p}]\dot{\phi}_a, \tag{13}$$

where $[G_a^{\ p}]$ denotes the first-order KIC matrix relating ϕ_p to ϕ_a.

According to the duality existing between the velocity vector and the force vector, the force relation between the independent joints and the dependent joints is described by

$$\mathbf{T}_a = [G_a^{\ p}]^{\mathrm{T}}\mathbf{T}_p. \tag{14}$$

Then, the effective load reference to the independent joints is given by

$$\mathbf{T}_a^* = \mathbf{T}_a + [G_a^{\ p}]^{\mathrm{T}}\mathbf{T}_p = [G_a^{\ \phi}]^{\mathrm{T}}\mathbf{T}_\phi, \tag{15}$$

where

$$[G_a^{\ \phi}] = \begin{bmatrix} I \\ [G_a^{\ p}] \end{bmatrix}, \tag{16}$$

$$\mathbf{T}_a = (T_1 \quad T_3)^{\mathrm{T}}. \tag{17}$$

In Eq. (15), $\mathbf{T}_\phi$ denotes a force vector consisting of $\mathbf{T}_a$ and the whole set or subset of the joint torque vector for the dependent joints.

2.3. Forward kinematics for a five-bar mechanism

Since the joint $({}_r\phi)$ of the rth chain is composed of some of the independent and dependent joints, ${}_r\dot{\phi}$ can be expressed in terms of the independent joints by

$${}_r\dot{\phi} = [{}^rG_a^{\ \phi}]\dot{\phi}_a, \tag{18}$$

where the matrix $[{}^rG_a^{\ \phi}]$ is formed by extracting some rows from $[G_a^{\ p}]$, augmented with a unity in the ith row and the jth column and with zeros in all other elements of the ith row if ${}_r\phi_i = \phi_{a_j}$. Thus, the forward kinematics for the common object is obtained by embedding the first-order internal KIC into one of the rth pseudo open-chain kinematic expressions as follows:

$$\dot{\mathbf{u}} = [{}_rG_\phi^{\ u}]{}_r\dot{\phi} = [G_a^{\ u}]\dot{\phi}_a, \tag{19}$$

where the forward Jacobian is determined by

$$[G^{u}_{a}] = [{}_{r}G^{u}_{\phi}][{}^{r}G^{\phi}_{a}]. \tag{20}$$

3. Kinematic optimal design for five-bar finger with redundant actuator

3.1. Optimization methodology

The given problem in this work is a nonlinear discrete optimization with constraints. To deal with this problem, three numerical methods are used. The exterior penalty function method is employed to transform the constrained optimization problem into an unconstrained optimal problem. Powell's method is applied to obtain an optimal solution for the unconstrained problem, and the quadratic interpolation method is utilized for uni-directional minimization [15].

3.2. Kinematic design indices

Based on the effective force relationship between the operational force vector and the input force vector, the ratio of the two-norm of the output load to that of the input load can be expressed as

$$\frac{\|\mathbf{T}_u\|}{\|\mathbf{T}_\phi\|} = \left\{ \frac{\mathbf{T}_\phi^{\mathrm{T}}[G^{\phi}_{u}][G^{\phi}_{u}]^{\mathrm{T}}\mathbf{T}_\phi}{\mathbf{T}_\phi^{\mathrm{T}}\mathbf{T}_\phi} \right\}^{1/2}, \tag{21}$$

where $\|\mathbf{T}_\phi\|$ and $\|\mathbf{T}_u\|$ are defined as

$$\|\mathbf{T}_\phi\|^2 = \mathbf{T}_\phi^{\mathrm{T}}\mathbf{T}_\phi, \tag{22}$$

$$\|\mathbf{T}_u\|^2 = \mathbf{T}_u^{\mathrm{T}}\mathbf{T}_u. \tag{23}$$

Based on the Rayleigh quotient, the output bounds with respect to the input loads are given as

$$\sigma_{\min}\,\|\mathbf{T}_\phi\| \le \|\mathbf{T}_u\| \le \sigma_{\max}\,\|\mathbf{T}_\phi\|, \tag{24}$$

where $\sigma_{\min}$ and $\sigma_{\max}$ are the square root of minimum and maximum singular values of $[G^{\phi}_{u}][G^{\phi}_{u}]^{\mathrm{T}}$, respectively. Since the nonzero eigenvalue of $[G^{\phi}_{u}]^{\mathrm{T}}[G^{\phi}_{u}]$ is the same as those of $[G^{\phi}_{u}][G^{\phi}_{u}]^{\mathrm{T}}$, the nonzero eigenvalues are obtained in terms of $[G^{\phi}_{u}]^{\mathrm{T}}[G^{\phi}_{u}]$, and these singular values are used in determining the bounds of the force transmission ratio. An alternative expression of Eq. (24) is

$$\frac{1}{\sigma_{\max}} \le \frac{\|\mathbf{T}_\phi\|}{\|\mathbf{T}_u\|} \le \frac{1}{\sigma_{\min}}, \tag{25}$$

where $\sigma_{\mathrm{F}}[=(1/\sigma_{\min})]$ is defined as the maximum force transmission ratio (i.e., actuator capacity for a unit operational load of $\|\mathbf{T}_u\|$).

3.2.1. Single design index

One of the basic aspects in manipulator design is determining the workspace. The operating region or workspace of the five-bar finger will be characterized by a reachable workspace. Also, a manipulator should be designed so that it has a well-conditioned workspace which allows its end-effector to move from one regular value to another without passing through a critical value (i.e., singularity). An isotropic index is a criterion to measure such phenomenon. The isotropic index, σ_{I}, is defined as the inverse of the condition number and provides a measure of the shape of the transmission ellipsoid. That is,

$$\sigma_{\mathrm{I}} = \frac{\sigma_{\min}}{\sigma_{\max}}. \tag{26}$$

The global isotropic index is defined with respect to the entire workspace of the manipulator as

$$\Sigma_{\mathrm{I}} = \frac{\int_W \sigma_{\mathrm{I}}\, \mathrm{d}W}{W}, \tag{27}$$

where the workspace of manipulators is denoted as

$$W = \int_W \mathrm{d}W. \tag{28}$$

The actuator capacity of the manipulator is another important design criterion. The maximum force transmission ratio is defined as the required actuator capacity for a unit operational load of $\|\mathbf{T}_u\|$. The global maximum force transmission ratio is defined with respect to the entire workspace of the manipulator as

$$\Sigma_{\mathrm{F}} = \frac{\int_W \sigma_{\mathrm{F}}\, \mathrm{d}W}{\int_W \mathrm{d}W}. \tag{29}$$

The design of a manipulator system can be based on any particular criterion. However, the single criterion-based design does not provide sufficient control on the range of the design parameters involved. Therefore, a multi-criteria based design has been proposed [11]. However, the previous multi-criteria methods did not provide any systematic design procedure and flexibility in design. In the light of these facts, a composite design index is proposed in the following section.

3.2.2. Composite design index

Several methodologies have been proposed to cope with multi-criteria based design, and the following equation is an example of a performance index which is constructed by combining several design indices, P_1, P_2, P_3, ... :

$$DI = C_1P_1 + C_2P_2 + C_3P_3 + \cdots, \tag{30}$$

where C_i denotes the weighting for the ith design index. In the above equation, however, various design indices are usually incommensurate concepts due to differences in unit and physical meanings, and, therefore, should not be combined with normalization and weighting functions unless they are transferred into a common domain. In other words, quantitative combination should be avoided. Instead, these design indices should be combined qualitatively. In consideration of this fact, a multi-criteria based design methodology employing a concept of a composite design index is introduced. As the first step to this process, preference information should be given to each design parameter and design index. Then, each design index is transferred to a common preference design domain, which ranges from zero to one. Here, the preference given to each design criterion is very subjective, according to the designer. Preference can be given to each criterion by weighting. This provides flexibility in design. For Σ_I, the best preference is given the maximum value, and the least preference is given the minimum value of the criterion. Then, the design index is transferred into a common preference design domain as below [12]

$$\tilde{\Sigma}_I = \frac{\Sigma_I - \Sigma_{I_{min}}}{\Sigma_{I_{max}} - \Sigma_{I_{min}}}, \tag{31}$$

where '$\sim$' implies that the index is transferred into a common preference design domain. Since the workspace is also in favor of the maximum value, the design index transferred into a common preference design domain is given as

$$\tilde{W} = \frac{W - W_{min}}{W_{max} - W_{min}}. \tag{32}$$

On the other hand, the force transmission ratio is in favor of the minimum value, and the design index transferred into the common preference design domain is given as

$$\tilde{\Sigma}_F = \frac{\Sigma_{F_{max}} - \Sigma_F}{\Sigma_{F_{max}} - \Sigma_{F_{min}}}. \tag{33}$$

Note that each composite design index is constructed such that a large value represents a better design. Large $\tilde{W}$ implies that the system possesses a large workspace, large $\tilde{\Sigma}_I$ implies that the system possesses a good isotropic characteristic within the given workspace, and large $\tilde{\Sigma}_F$ implies that the system requires a small actuator effect to support a unit operational load within the given workspace.

A set of optimal design parameters is obtained based on the max–min principle [16]. Initially, the minimum values among the design indices for all sets of design parameters are obtained, and then a set of design parameters, which has the maximum of the minimum values, is chosen as the optimal set of design parameters. Based on this principle, the composite global design index (CGDI) is

defined as the minimum value of the above-mentioned design indices at a set of design parameters, and is given as

$$\mathrm{CGDI} = \min\{\tilde{W}^{\alpha}, \tilde{\Sigma}_{\mathrm{I}}^{\beta}, \tilde{\Sigma}_{\mathrm{F}}^{\gamma}\}. \tag{34}$$

The upper Greek letters (α, β, γ) represent the degree of weighting, and usually a large value implies large weighting. In general, the value of weighting is determined based on a fuzzy measure such as normal, very, more or less, absolutely and so on [16]. In order to evenly satisfy the several design objectives for all design indices, all of the weighting factors are set to 1.0. Now, a set of optimal design parameters is chosen as the set that has the maximum CGDI among all CGDIs calculated for all sets of design parameters.

3.3. Kinematic optimization

The link lengths and the base width of the five-bar mechanism can be cited as kinematic design parameters. Initially, we assume that the workspace of the five-bar mechanism is the first quadrant of the x–y plane. That is,

$$0.01\ \mathrm{m} \leq x,\ y \leq 0.3\ \mathrm{m}. \tag{35}$$

Now, kinematic constraints associated with these parameters are given as

$$l_1 + l_2 = 0.3\ \mathrm{m}, \tag{36}$$

$$l_3 \geq 0.07\ \mathrm{m}, \tag{37}$$

$$l_4 \geq 0.07\ \mathrm{m}, \tag{38}$$

$$l_5 \geq 0.02\ \mathrm{m}, \tag{39}$$

where l_1 and l_2 are decided based on the range of the workspace. Also, l_3 and l_4 should be greater than the minimum link length which is decided based on the size of the transmission system embedded inside the link. l_5 requires a minimum length to attach a finger-tip at the end of the link.

Kinematic optimization for the five-bar mechanism has been performed for the case of $\alpha = 1$, $\beta = 4$, $\gamma = 1$, in which a large weighting is given the isotropic index, and for the case of $\alpha = 1$, $\beta = 1$, $\gamma = 4$, in which a large weighting is given the maximum force transmission ratio. Optimization has been performed for several initial points to guarantee the global minimum. In Table 1, some of the optimization results for the minimum and redundant actuating cases are shown. Kinematic characteristics resulting from the optimization procedure have been improved in comparison to those of the non-optimized case in which all link lengths are chosen as a unit length. We can conclude that, for the minimum actuation case, actuation of the first and fourth joints (here, we denote it as 14)

has the best performance in both the isotropic and maximum force transmission characteristics, that for one redundant actuation case (i.e., three actuators), actuation of the first, fourth, and fifth joints (here, we denote it as 145) has the best performance in both characteristics, and that for two redundant actuation cases (i.e., four actuators), actuation of the first, third, fourth, and fifth joints (here, we note it as 1345) has the best performance in both characteristics.

In general, the force transmission characteristic enhances as the number of redundant actuator increases, while the motion isotropy deteriorates. This result denotes a trade-off between the force and motion isotropy. Therefore, a guideline to how many redundant actuators are appropriate is necessary. In order for this, we simultaneously analyze the optimized result of the motion isotropy along with the workspace. From Fig. 2(a) and (b), it is shown that the case of one redundant actuator possesses the largest workspace for both the isotropic index (Σ_I) and the force transmission ratio (Σ_F), while the cases of two or three redundant actuators have smaller workspaces, especially for the maximum force transmission ratio. Therefore, we can conclude that many redundant actuators do not always

Table 1
Optimization results

Actuating joints	Case	W_{area}	Σ_I	Σ_F
13	Initial set	5.76	0.1757	4.5294
	Isotropic optimization	5.19	0.4990	2.2001
	Force transmission optimization	3.10	0.4328	1.9885
14	Initial set	5.76	0.4468	1.9720
	Isotropic optimization	2.76	0.6676	1.2828
	Force transmission optimization	3.17	0.4759	1.1810
34	Initial set	5.76	0.4129	2.2236
	Isotropic optimization	5.12	0.6967	1.9118
	Force transmission optimization	5.50	0.5583	1.5601
123	Initial set	5.76	0.2002	2.4400
	Isotropic optimization	4.92	0.5775	1.5406
	Force transmission optimization	2.49	0.5014	1.4832
134	Initial set	5.76	0.3920	1.5632
	Isotropic optimization	2.78	0.5713	1.2562
	Force transmission optimization	4.30	0.4598	1.1634
145	Initial set	5.76	0.4243	1.5554
	Isotropic optimization	4.75	0.6471	1.0702
	Force transmission optimization	4.40	0.5812	1.0008
1345	Initial set	5.76	0.3723	1.4693
	Isotropic optimization	5.66	0.6363	1.0538
	Force transmission optimization	3.13	0.5318	0.7400
12345	Initial set	5.76	0.3277	1.3235
	Isotropic optimization	5.26	0.6397	0.8204
	Force transmission optimization	3.29	0.5289	0.6996

guarantee performance enhancement of the system, and one judicial choice of a redundant actuator greatly improves the general performances of the system.

Fig. 3 illustrates the optimal five-bar configurations for some cases. The black dots denote the positions of the actuators. Also, in order to visualize the performance enhancement after optimization, the overall trends of the kinematic isotropic index and the maximum force transmission ratio for optimized and non-optimized cases are shown in Figs. 4 and 5. As expected, optimization results in reduction (i.e., enhancement) of the maximum force transmission ratio and the improvement of the kinematic isotropy throughout the workspace.

Although the kinematic isotropy and the maximum force transmission ratio, along with the workspace of the system, are considered in the above, the maximum force transmission ratio is believed to be a much more important factor than the kinematic isotropy and the workspace, especially for fingers in multi-fingered hands, because they usually require a large payload and are operated in a small workspace. Specifically, the value of the force transmission ratio for 145 joints has been reduced by as much as 15.3% of that of 14 joints, and the value of the force transmission ratio for 1345 joints has been reduced by as much as 37.3%

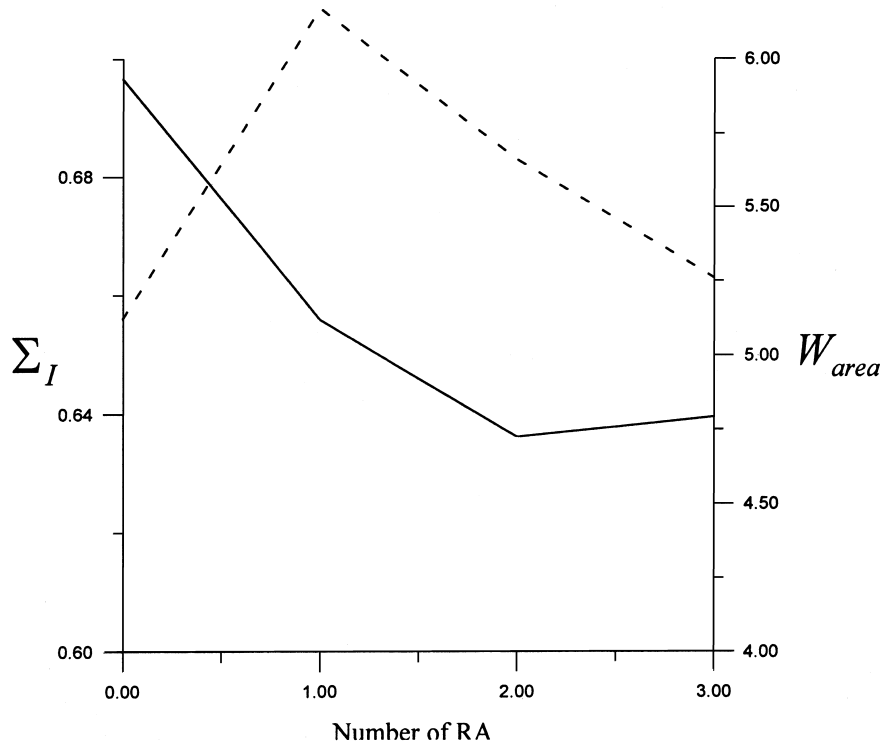

Fig. 2. Performance measure for Σ_I, Σ_F and W_{area} (dashed line) with respect to the number of redundant actuators. (a) Comparison of Σ_I (solid line) and W_{area} (dashed line). (b) Comparison of Σ_F (solid line) and W_{area} (dashed line).

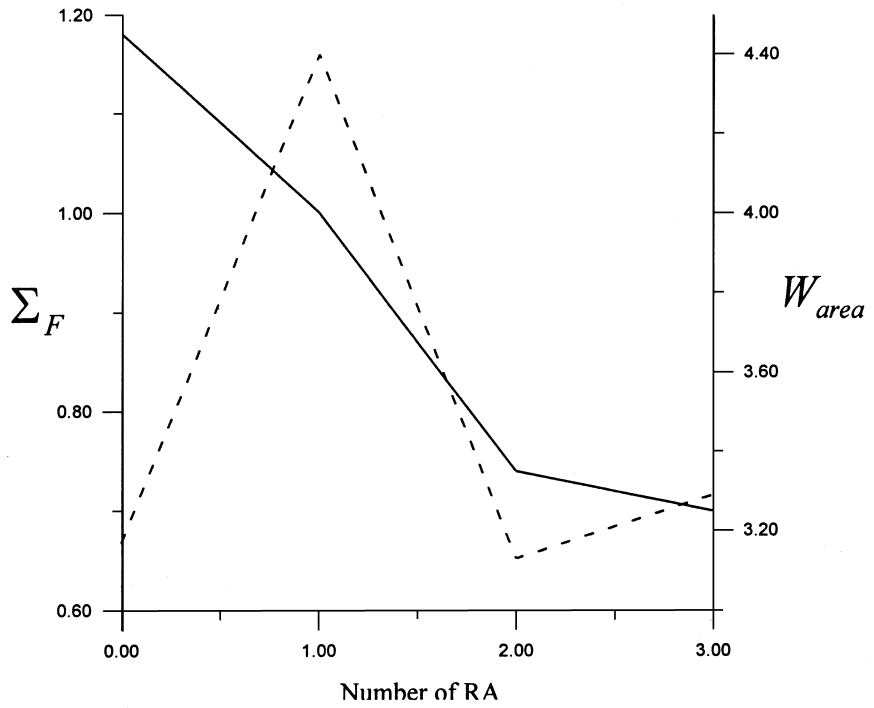

Fig. 2 (*continued*)

of that of 134 joints, and the value of the force transmission ratio for full actuation (i.e., 12345 joints) has been reduced much more than the two previous cases. Conclusively, two redundant actuations (i.e., 1345 joint actuation) are suggested to enhance the force transmission ratio of the five-bar mechanism in the expense of the small workspace, while one judicial choice of the redundant actuator improves the general performance of the finger system the best.

4. Development of the five-bar finger with a redundant actuator

4.1. Structure of the five-bar finger

Fig. 6 shows the prototype of the five-bar mechanism. According to the optimization result, four actuators are placed to 1345 joints. Each joint of the finger is driven by a compact actuator mechanism having an ultrasonic motor and a gear set with a potentiometer, and the system is controlled by a VME bus-based control system. The ultra-sonic motors have a high torque/size ratio, as compared to a DC motor with a similar size [17]. A gear transmission having about a 15:1 speed reduction ratio is employed. Particularly, the gear transmission consisting of

a series of spur gears and the potentiometer is embedded inside the link, which yields a compact and modular design of the finger mechanism. Using this mechanism, several internal force control algorithms developed in previous works associated to the five-bar finger mechanism [6,7], are to be experimentally verified.

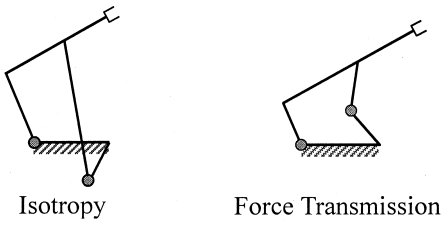

Optimized Configurations for 1· 4 Joint Actuation

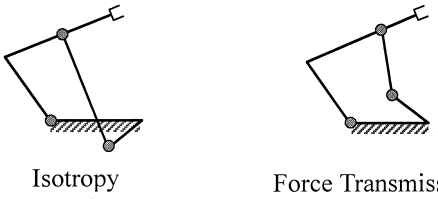

Optimized Configurations for 1· 4· 5 Joint Actuation

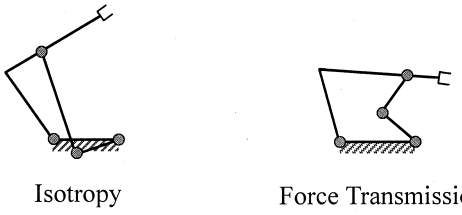

Optimized Configurations for 1· 3· 4· 5 Joint Actuation

Fig. 3. Optimal finger configurations.

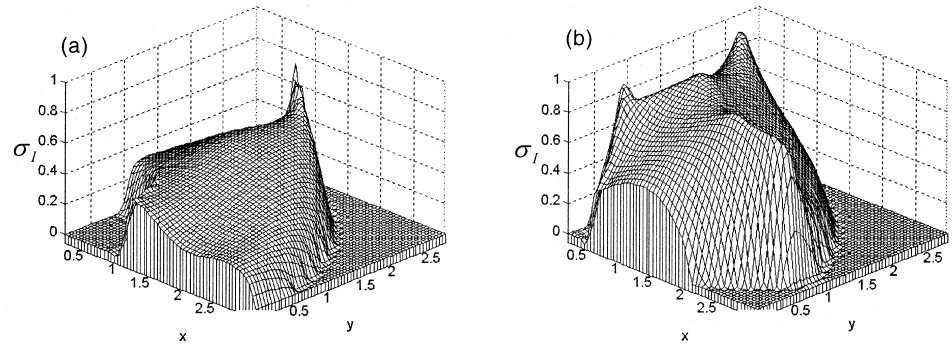

Fig. 4. Comparison of isotropy before and after optimization. (a) Isotropy before optimization for 345 joint actuation. (b) Isotropy after optimization for 345 joint actuation.

5. Conclusions

In this paper, we proposed employment of a redundant actuation in a finger design with the purpose of enhancing the kinematic isotropic characteristic and maximum force transmission ratio of the finger mechanism. Using the concept of a composite design index, which allows multi-purpose and multi-variable optimization, optical sets of actuator locations and link lengths for the cases of using the minimum numbers of actuators, one-, two-, and three-redundant actuators are obtained. Three design indices such as the workspace, the isotropic index, and the force transmission ratio were simultaneously optimized with consideration of the relative weighting factors. According to the optimization result, several finger-configurations optimized for the special performance index are illustrated, and it is concluded that the case of one redundant actuator is the most effective in comparison to the cases of more redundant actuators, and that the case of two redundant actuators is the most effective in a multi-fingered

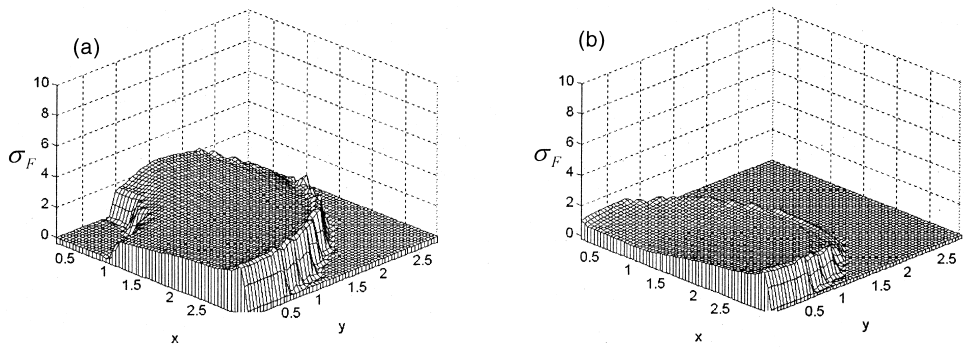

Fig. 5. Comparison of force transmission ratio before and after optimization. (a) Force transmission ratio before optimization for 345 joint actuation. (b) Force transmission ratio after optimization for 345 joint actuation.

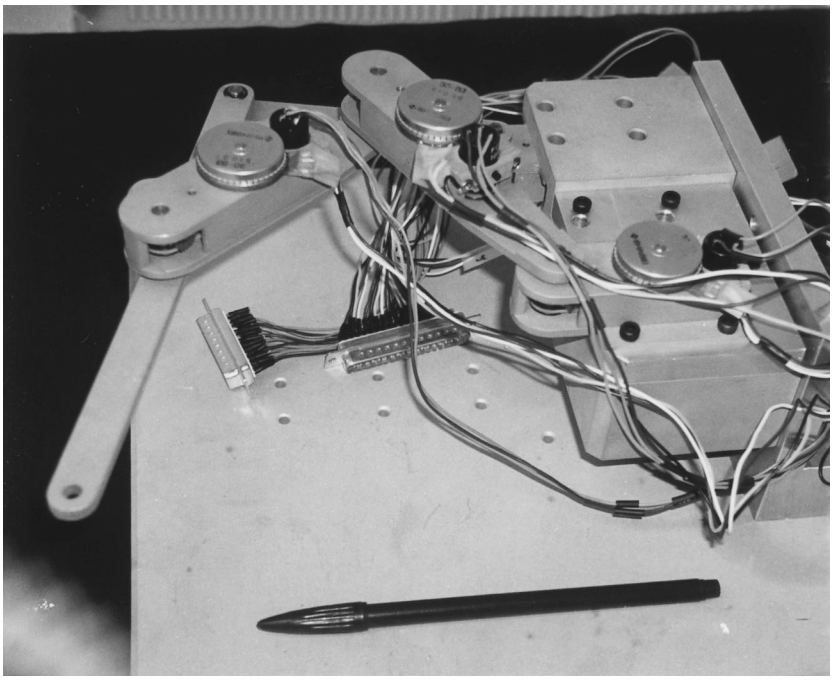

Fig. 6. Prototype of five-bar finger mechanism.

operation in which the force characteristic is relatively important, as compared to the workspace. Future work involves experimental work, associated with the internal force control and development of a three-fingered hand made of a five-bar finger mechanism.

Acknowledgements

This work has been supported by the Korea Institute of Science and Technology 2000 Human Robot program.

References

[1] Jacobson SC, Wood JE, Knutti DF, Biggers KB. The Utha/MIT dexterous hands. Int Journal of Robotics Research 1984;3(4):21–50.
[2] Loucks CS, Johnson VC, Boissiere PT, Starr GP, Steele JPH. Modeling and control of the standfor/JPL hand. In: IEEE Proceedings on Robotics and Automation Conference, 1987. p. 573–8.
[3] Lin L-R, Huang H-P. Mechanism design of new multi-fingered robot hands. In: IEEE Proceedings on Robotics and Automation Conference, 1996. p. 1471–6.

[4] Buss M, Kleinmann KP. Multi-fingered grasping experiments using real-time grasping force optimization. In: IEEE Proceedings on Robotics and Automation Conference, 1996. p. 1807–12.
[5] Spence PA. Basic human anatomy. The Benjamin/Cummings Publishing Co Inc, 1986.
[6] Yi B-J, Suh IH, Oh S-R. Analysis of a five-bar finger mechanism having redundant actuators with applications to stiffness and frequency modulation. In: IEEE Proceedings on Robotics and Automation Conference, 1997. p. 759–65.
[7] Yi B-J, Oh S-R, Suh IH, You BJ. Synthesis of actively adjustable frequency modulators: the case for a five-bar finger mechanism. In: IEEE/RSJ Proceedings on IROS, 1997. p. 1098–104.
[8] Nakamura Y, Ghodoussi M. Dynamic computation of closed-link robot mechanisms with nonredundant and redundant actuators. IEEE Journal of Robotics and Automation 1989;5:294–302.
[9] Nahon MA, Angeles J. Force optimization in redundantly-actuated closed kinematic chains. In: IEEE Proceedings on Robotics and Automation Conference, 1989. p. 951–6.
[10] Kumar VJ, Gardner J. Kinematics of redundantly actuated closed-chain. IEEE Journal of Robotics and Automation 1990;6:269–73.
[11] Kurz R, Hayward W. Multiple-goal kinematic optimization of a parallel spherical mechanism with actuator redundancy. IEEE Journal of Robotics and Automation 1992;8:644–51.
[12] Lee SH, Yi B-J, Kwak YK. Optimal kinematic design of an anthropomorphic robot module with redundant actuators. Mechatronics 1997;7(5):443–64.
[13] Kang HJ, Yi B-J, Cho W, Freeman RA. Constraint-embedding approaches for general closed-chain system dynamics in terms of a minimum coordinate set. The 1990 ASME Biennial Mechanism Conference 1990;DE-24:125–32.
[14] Freeman RA, Tesar D. Dynamic modeling of serial and parallel mechanisms/robotic systems: Part I — Methodology, Part II — Applications. In: Proceedings of the 20th ASME Mechanisms Conference, Orlando, FL, 1988.
[15] Luenberger DG. Linear and nonlinear programming. 2nd ed. Addison Wesley, 1989.
[16] Terano T, Asai K, Sugeno M. Fuzzy systems theory and its applications. 1st ed. San Diego: Harcourt Brace Jovanovitch, 1992.
[17] Kato A, Ito K, Ito M. Adjustable compliance motion of an ultrasonic motor. Int Journal of Robotics and Automation 1993;5(5):434–7.